Vertical Optokinetic Eye Movements in the Larval Zebrafish

David-Samuel Burkhardt*[1], Gabriel Möller*[1], Laurian Deligand[1,2], Christiane Fichtner[1,3], Tim C. Hladnik[1,4], Aristides B. Arrenberg[1]

*these authors contributed equally

[1] Werner Reichardt Centre for Integrative Neuroscience and Institute for Neurobiology, University of Tuebingen, 72076 Tuebingen, Germany

[2] Biology Department, Ecole Normale Superieure, PSL Universite Paris

[3] Faculty of Medical and Life Sciences, University of Applied Sciences Furtwangen

[4] Graduate Training Centre of Neuroscience, University of Tuebingen, 72076 Tuebingen, Germany

Corresponding author email address: aristides.arrenberg@uni-tuebingen.de

Abstract

The optokinetic response (OKR), a reflex enabling stable visual processing by minimizing retinal slip, has been well characterized in fish over the last decades, leading to insights and a better understanding of the underlying neuronal control and circuitries. However, only the horizontal component of the OKR has been investigated so far, although the optokinetic response is not limited to the horizontal plane, as it has also been observed vertically and even torsionally in other species. In this study, we characterize the vertical optokinetic response (vOKR) in larval zebrafish and compare it to the horizontal OKR (hOKR) and the vertical vestibulo-ocular reflex (vVOR). Two custom-built experimental setups, allowed for controlled vestibular stimulation alongside precise eye tracking and simultaneous recording of both horizontal and vertical eye movements during visual stimulation. Our findings reveal a distinct vOKR in larval zebrafish, but with a much smaller dynamic range compared to the hOKR and without any quick phases (resetting saccades). When presented with constant roll-rotating visual stimuli, zebrafish exhibit a brief initial vertical eye rotation in the direction of the stimulus, followed by a period with no further rotation but interspersed with only spontaneous saccades. This behavior contrasts sharply with the periodical occurrence of resetting saccades during hOKR. Despite its limited dynamic range, the initial vertical response is tuned to similar spatial frequencies and angular velocities as the hOKR. Intriguingly, zebrafish are capable of large vertical eye movements during the vVOR, suggesting that the restricted dynamic range of the vOKR is not due to inherent motor limitations. While it is unclear whether the observed differences in vertical versus horizontal optokinetic control have an adaptive value for zebrafish, the identified differences are drastic and informative for further studies on oculomotor circuits.

Introduction

Eye movements are ubiquitous and essential in vertebrates, enabling animals to stabilize their gaze and process visual information efficiently. Investigation of eye movements provides valuable insights into the neural circuitry underlying sensory perception, motor coordination, and behavior. In all vertebrates, eye movements are controlled by six extraocular muscles that enable horizontal (yaw), torsional (pitch), and vertical (roll) rotations [1]. It is well-established in mammals that these three directions of eye movements are used to counteract visual movements based on either vestibular or visual input, thereby stabilizing gaze position and minimizing retinal slip. In mammals all of those three directions of eye movements are used to counteract visual motion based on either vestibular or visual input to stabilize gaze position.

Visual gaze stabilization is mediated via the optokinetic response (OKR) to large-field visual motion. This reflex is exhibited across vertebrate species and consists of two components: a slow phase which involves relatively slow following of the visual stimulus by the eye and a resetting quick phase (also called saccade), which moves the eye in the opposite direction of the stimulus once the maximum eye excursion is reached. The speed during the slow phase can be related to stimulus speed to calculate the gain and thus indicates how successfully the eye movement counteracts retinal slip. The OKR is often used as an assay to gain insight into visual processing and oculomotor circuits, which is well researched for the horizontal, vertical and torsional plane in mammals [2–5].

The larval zebrafish is a powerful model system for studying eye movements and their underlying circuitries [6,7]. This species combines a fully functional visual system, with the 6 eye muscles needed for movement in all directions [8,9], and a vestibular system that enables eye movements in response to acceleration and orientation within a gravitational field [10–13]. Zebrafish also offer unparalleled optical accessibility and genetic tools, making them an ideal organism for dissecting oculomotor circuits [14]. While previous studies have extensively characterized horizontal [11,15–18] and occasionally torsional [19] eye movements in larval zebrafish, vertical eye movements, including the vertical optokinetic response (vOKR), have been largely overlooked in teleosts and only little is known about their expression and underlying circuitry. Vertical eye movements in response to vestibular input have been studied in larval xenopus [12] and larval zebrafish [20], and in archer fish 3D-motions of eyes, including vertical movements, can be measured with a stereo camera setup [21]. Furthermore, the dorsal light reflex (DLR), a behavior in which fish orient their dorsal body side to the direction of maximum light intensity, has been described to also occur as vertical eye movements towards the direction of brightest illumination in immobilized goldfish [22]. However, the characterization

of vOKR in teleosts - especially in zebrafish - is missing despite the fact that these aquatic animals readily navigate in 3D in the water column and are able to move their eyes vertically.

Both optokinetic and optomotor responses stabilize fish gaze and posture based on optic flow mediated self-motion estimation [23–28]. This optic flow is mainly processed in the optic tectum and pretectum by making use of a diverse set of neurons, tuned to different directions and motion patterns. Each direction-selective neuron prefers one out of four local directions: up, down, temporal-nasal (TN), and nasal-temporal (NT) motion [27,29–31]. Although zebrafish are thought to predominantly experience horizontal motion (TN and NT) and only small vertical shifts due to their swimming behavior [32], surprisingly the number of neurons which are direction- selective for vertical up and down motion is approximately equal to those encoding horizontal motion [27,31]. Therefore, vertical motion, be it pure up/down translation, left/right roll, seems to be relevant for zebrafish.

In this study we simultaneously record horizontal and vertical eye movements in 4 days-old zebrafish larvae (4 days post fertilization, dpf) while eliciting both horizontal and vertical OKR (hOKR and vOKR) by visual stimulation. Further, we quantify the vertical vestibular-ocular response (vVOR), a reflex that works in concert with the OKR and relies on information from the semicircular canals and otoliths to respond to head velocity. We compare the vVOR dynamics to those of the vOKR. We show that vOKR does exist in larval zebrafish, but its characteristics strongly differ from those of the hOKR. Understanding and comparing both horizontal and vertical eye movements is essential for further investigations into the neural circuits driving zebrafish oculomotor behavior, especially with regard to optic flow. The following study provides a behavioral characterization of the vOKR in larval zebrafish for further exploration of the role and relevance of direction-selective neurons during vertical motion, their associated neuronal networks and last but not least their significance in relation to zebrafish behavior.

Results

vVOR has a large dynamic range and is driven by rotational head position

To demonstrate that larvae are capable of large vertical eye movements, we first performed vVOR experiments. Animals were mounted in 1.6 % agarose in a setup that allowed controlled rotations about the caudo-rostral axis (clockwise and counter-clockwise roll; CW and CCW) alongside tracking of vertical eye movements. Vertical eye movements were recorded in the

dark via a camera placed on the same rotation axis (Figure 1A). Three different angular velocities (22.5 °/s, 45 °/s and 90 °/s) were tested to examine vertical eye movements elicited by vestibular input. In total N = 9 larvae were used in this experiment. Throughout the experiments, the larvae exhibited a nearly perfect sinusoidal pattern of vertical eye position changes in response to the full rotations about the caudo-rostral axis, with the maximal eye deflection occurring at 90° and 270° head positions (Figure 1B). Occasionally, the eye traces contained small outliers, which could be traced back to irregularly occurring vibrations of the stepper motor driving the setup.

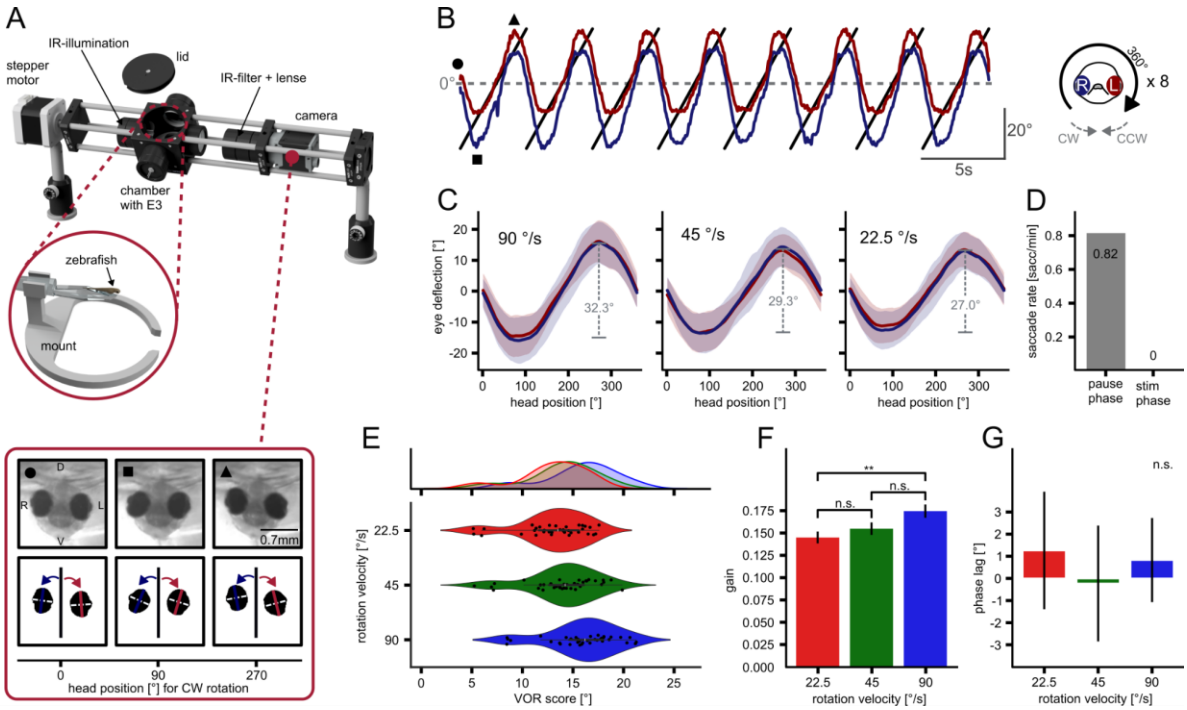

Figure 1: Investigating the vertical vestibulo ocular reflex. (A) Schematic of the experimental setup (KEBAB) used to examine vertical eye movements during constant rotation of the fish (KEBAB is an abbreviation for Kinematic Evaluation of Behavior during Animal Body Roll). The setup was driven by a stepper motor and controlled via the open-source software vxPy. Bottom: illustration of tracking vertical eye movements. **(B)** Raw eye traces of the left and right eye during rotation at 90°/s. The symbols (dot, square and triangle) indicate the eye position displayed in panel A). One stimulation phase contained 8 full rotations either CW or CCW. **(C)** Stimulus triggered average (STA) of eye positions during full rotation at 90°/s, 45°/s and 22.5°/s for all stimulations phases and across all fish (n = 9). Envelopes show the standard deviation. Grey dashed lines indicate the dynamic range. **(D)** Saccade rate during rotation and pause phase. **(E)** VOR score for 90°/s, 45°/s and 22.5°/s. VOR score only contained eye movements at the head rotation frequency. **(F)** Gain as ratio of sinus-fitted eye position to head position. **(G)** Phase lag as temporal difference between sinus-fitted eye position to head position. All p-values derived from paired t-test followed by Bonferroni-correction.

The average dynamic range of both eyes increased with head velocity, reaching a maximum at 90 °/s (32.3 ° ± 6.4 °; 29.3 ° ± 6.2 ° and 27.0 ° ± 5.9 ° for 45 °/s and 22.5 °/s, respectively;

mean ± SD) (Figure 1C). Interestingly, the larvae did not perform any saccades during the head rotations, while the saccade rate during the pause phases, when no rotation was performed, was 0.82 saccades/min (Figure 1D). To analyze only the components of the vertical eye movements relating to the stimulus frequency, Fourier analysis was performed to calculate the VOR score. The VOR scores for all angular velocities were nearly normally distributed, with means of 15.9 ° ± 3.4 °, 13.9 ° ± 3.4 °, and 13.0 ° ± 3.3 ° (mean ± SD for 90 °/s, 45 °/s and 22.5 °/s angular velocity), and differed with regard to the angular velocities (Figure 1E). The fact that the vVOR score (15.9, 13.9 ° and 13.0 °; mean) and the dynamic range half amplitude (16.2 °, 14.7 °, 13.5 °; mean) were close to each other indicates that the eye movements were almost solely driven by the rotational head position. The vVOR gain revealed differences across the angular velocities, peaking at 0.17 for 90 °/s (Figure 1F). The phase lag, however, contained both positive and small negative values close to zero, suggesting that the eyes nearly simultaneously moved together with the head, with almost no delay (Figure 1G). The small negative values can be explained by measurement inaccuracies and noise due to the stepper motor vibrations.

vOKR has much smaller dynamic range than hOKR and vertical quick phases are absent

To investigate the existence and function of the vOKR in zebrafish, a horizontally striped black and white pattern was rotated vertically around the fish at a constant angular velocity. Eye movements were tracked in two dimensions using top and front cameras to record both horizontal and vertical eye movements (Figure 2A). Various angular velocities and spatial frequencies were tested to assess the vOKR. Each combination of stimulus parameters was presented for 60 seconds, followed by a 60-second pause phase (Figure 2B). When presented with a constantly rotating vertical optokinetic stimulus, the zebrafish larvae did not exhibit the typical pattern of slow and quick phases observed in the hOKR. Instead, the eyes followed the visual stimulus for the first 4-5 seconds, reaching a plateau-like position from which they did not move further. This “start response” was primarily visible in the frontal camera, suggesting it was limited to the vertical component (Figure 2C). After reaching the plateau, the eyes began performing spontaneous saccades in both clockwise and counter-clockwise directions, which were visible in both the frontal and top cameras, indicating these saccades might have both vertical and horizontal components (Figure 2B). Between the spontaneous saccades, the eyes remained stationary or slowly drifted back towards a more neutral position. To visualize this surprising “start response” behavior, we compared the beginning phases of vOKR and hOKR (Figure 2D). For hOKR we used the same stimulus protocol but with vertical stripes and horizontal instead of vertical rotation (Figure 2D). When removing all saccades during vertical

and horizontal OKR and calculating the average cumulative eye trace during stimulation, the hOKR revealed the well-known constant slope in the direction of the stimulus, while the vOKR flattened out after about 4-5 seconds. Vertical eye movements during the horizontal stimulus protocol were also apparent, as observed in the front camera (Figure 2D).

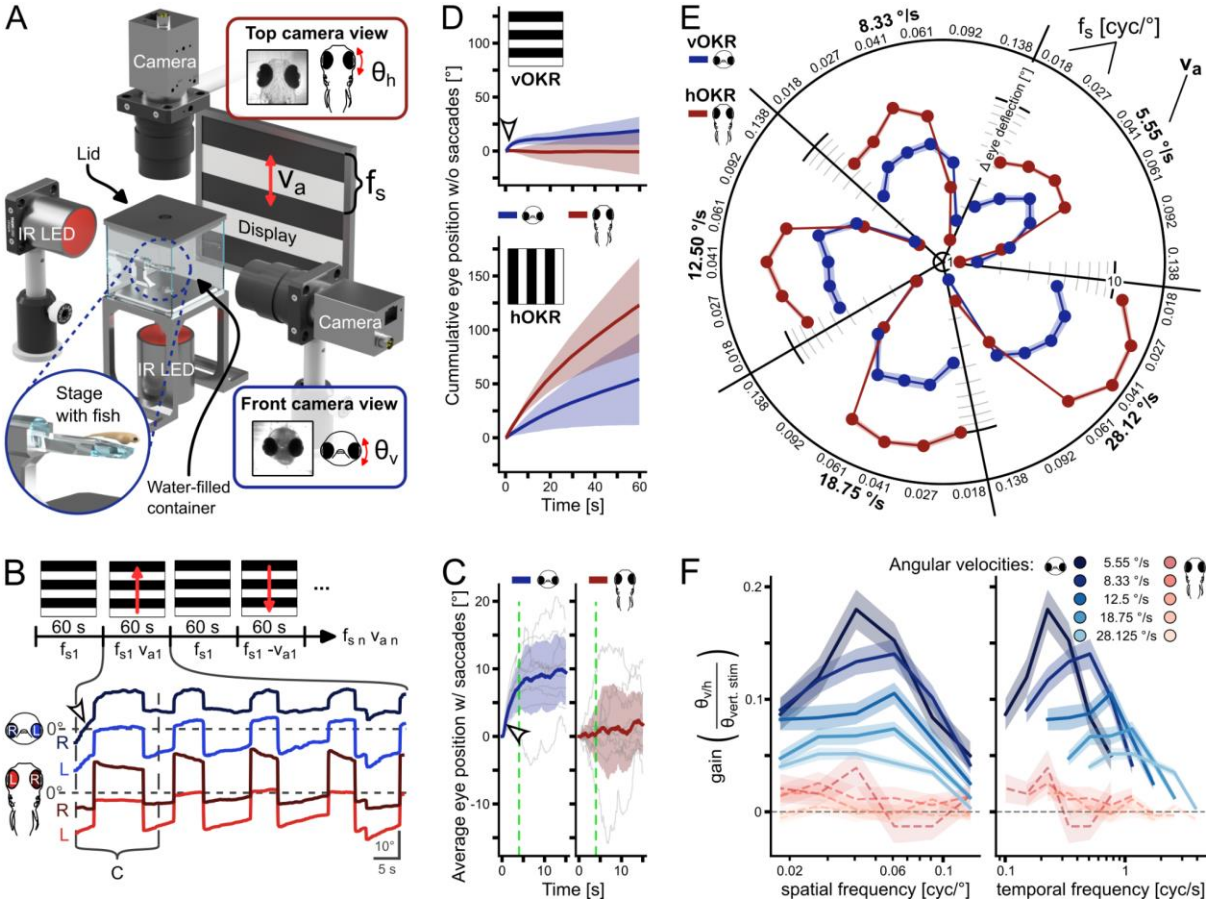

Figure 2: No vertical quick phases after initial zebrafish vOKR. (A) Schematic of the setup with two cameras simultaneously recording the horizontal (top) and vertical (front) eye movements. The second display on the right side of the fish is not shown in this illustration. **(B)** Stimulus protocol and example vertical (blue) and horizontal (red) eye traces of one stimulation phase of one fish. During the first seconds, only the vertical eye trace shows a deflection (arrowhead). **(C)** Average eye position of all fish and all visual stimulations for the first 15 s. Vertical eye trace (blue) shows a distinct rise (arrowhead) in the first 4 seconds (green dashed line) while the average horizontal eye position (red) does not change during vOKR. **(D)** Average cumulative eye position with saccades removed for vOKR (top) and hOKR (bottom) stimuli. The vertical start response is visible (arrowhead). Blue lines indicate front camera readings (vertical eye trace), red lines horizontal eye traces. **(E)** Mean amplitude within first 4 s after stimulus onset and standard error of the mean for each stimulus parameter pair. Blue: vertical amplitude for vOKR, red: horizontal amplitude for hOKR. **(F)** Gain tuning to spatial frequency and temporal frequency for all different angular velocities (symbols). Lines show mean and standard error of the mean. Blue: gain for vertical eye trace for vOKR stimulation. Red: gain calculated for horizontal eye trace for vOKR stimulation. Dashed horizontal line indicates a gain of 0. n = 10 fish.

The presence of larger eye position changes in the front camera during hOKR suggests that larval zebrafish either perform a small vertical component during the hOKR or that the projection of the eye onto the front camera is systematically affected by horizontal eye position changes. For the vOKR, horizontal eye position (measured by the top camera and removing saccades) remained stable around zero during vertical eye movements (Figure 2D). To examine the tuning of the start response during vOKR for different spatial frequencies and angular velocities, and to compare it to the tuning of hOKR, the eye position amplitude (half the dynamic range) and the gain were calculated after the first 4 seconds of stimulation, where eye deflection reached the previous described plateau. The dynamic range tuning was quite similar for vOKR and hOKR (Figure 2E). For all angular velocities, the dynamic range was around zero for the highest spatial frequency of 0.128 cyc/°, then increased with lower spatial frequency until reaching a maximal deflection for either 0.061 cyc/° or 0.041 cyc/° (hOKR and vOKR respectively) before starting to decline again. Additionally, the dynamic range of eye positions increased with angular velocity, with the dynamic range during hOKR being more narrowly tuned than during vOKR. The maximum amplitude for hOKR after 4 s was 16.92 ° ± 0.61 ° (at 28.12 °/s and 0.041 cyc/°), and 5.81 ° ± 0.38 ° for vOKR (at 28.12 °/s and 0.027 cyc/°).

The vOKR gain was generally higher for slower angular velocities (Figure 2F). Within a single angular velocity, the gain showed unimodal tuning in the range from 0.018 cyc/° to 0.128 cyc/° and peaked at medium spatial frequencies around 0.04 to 0.06 cyc/°. The same pattern held true when comparing the gain to temporal frequencies, where the slower the angular velocity, the lower the temporal frequency that elicited the highest gain. To further confirm that the eye movements recorded within the first seconds of stimulation only contained a vertical OKR, the gain was also calculated for the horizontal eye movements during vOKR stimulation. The resulting values all lay around zero, indicating no notable horizontal component was present in the early part of the vOKR.

vOKR shows phase advances and lags depending on the time period to stimulus reversal

Since the constant roll-rotating visual stimulus only elicited a transient vOKR within 4-5 seconds, a second sinusoidal rotation stimulus was used to extend the duration for which the eyes would follow the visual motion. The stimulus contained the same striped black and white pattern, but the rotation velocity followed a sinusoidal profile (Figure 3A). As a result, the stimulus slowly gained speed in one direction until reaching the maximum angular velocity, then decreased again until coming to a full stop before accelerating in the opposite direction. This stimulus introduced a new parameter, the repetition rate (rr), which indicated the frequency of the sinusoidal velocity envelope and provided information on how quickly the

maximum velocity was reached. Overall, the sinusoidal stimulus elicited sinusoidal vertical eye movements corresponding to the stimulus position, while no stimulus-associated horizontal eye movements were visible in the top camera. During stimulation, larvae showed spontaneous horizontal saccades that also led to deflections in the vertical eye position, but did not disrupt the overall sinusoidal pattern. Just as for the constantly rotating stimulus, no vertical resetting quick phases could be observed in response to the sinusoidal stimulus (Figure 3B).

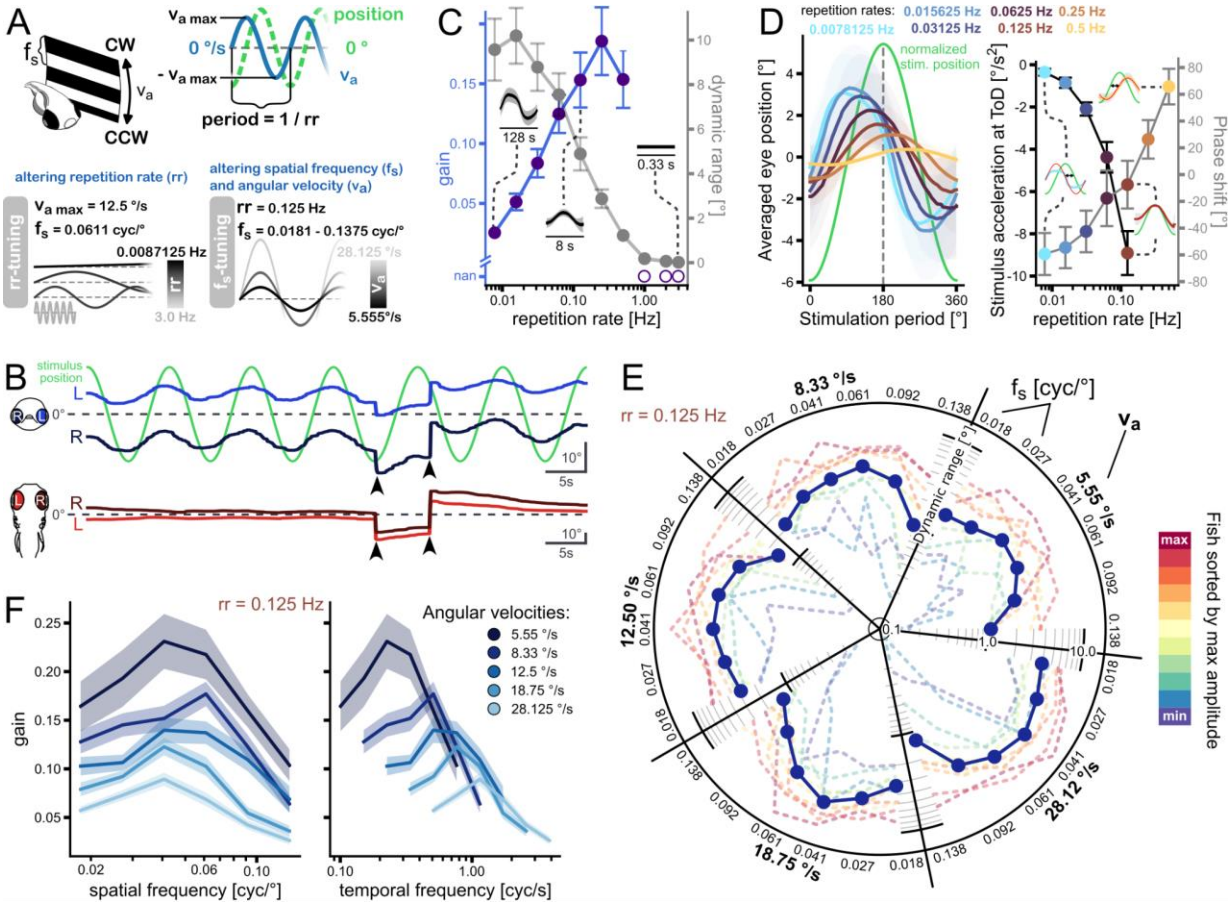

Figure 3: vOKR tuning to stimuli with sinusoidal velocity envelope. (A) Sinusoidal rotation stimulus scheme. Two different sinusoidal stimuli were used. In the rr tuning stimulus, the maximum angular velocity and the spatial frequency were constant while different repetition rates were tested. In the f_s tuning stimulus, the repetition rate was kept constant while spatial frequency and angular velocity were altered. CW: clockwise, CCW: counterclockwise, v_a: angular velocity, rr: repetition rate, f_s: spatial frequency. **(B)** Example recording with vertical (blue) and horizontal (red) eye traces. Spontaneous saccades during the sinusoidal response did not disturb the response but shifted it by the amplitude of the saccade (arrowheads). Note: different y-axis scales. **(C)** Mean and standard error of gain (blue) and full dynamic range (grey) over repetition rate. Insets show average response to one stimulus period over all fish for repetition rates 3.0 Hz, 0.125 Hz, and 0.0078125 Hz (n = 8 fish). **(D)** Left: Average response to one stimulus period for different repetition rates. The timescale is normalized to one stimulus period. Vertical dashed line indicates turning point of stimulus position. Right: Phase lag of the vOKR (gray lines) for different repetition rates; and acceleration value of the stimulus (black lines) at the timepoint of eye movement direction change (phase lag). Datapoints are color-coded with respect to their repetition rate and show mean and standard deviation. Insets show example average responses to one stimulus period of one fish. Green curve indicates stimulus position, red curve shows sine fit to average eye trace. Black arrows indicate the phase shift between stimulus and average response. **(E)**

Dynamic range for each stimulus parameter set. Datapoints indicate mean of all fish (n = 11 fish). Dashed lines show mean dynamic range of single fish, colored according to their mean amplitude. **(F)** Mean gain with standard error over spatial frequency (left) and temporal frequency (right) for all different angular velocities (see color legend).

We tested different repetition rates while keeping the maximum angular velocity constant (12.5 °/s) and using only one spatial frequency close to the optimum (0.061 cyc/°). The parameters were similar to those used by Dehmelt et al. (2021) for horizontal OKR [18]. For repetition rates between 0.5 Hz and 0.0078 Hz, vertical eye positions followed the stimulus. Repetition rates greater than 0.5 Hz did not elicit any response (Figure 3C). The gain was calculated as the ratio of the amplitude of a fitted sinusoidal function to the eye position and the stimulus position. The gain was relatively high for repetition rates between 0.5 Hz and 0.125 Hz (maximum of 0.19 at 0.25 Hz) but started to decrease for lower repetition rates until reaching a value of 0.03 (at 0.0078 Hz) (Figure 3C). However, the eye traces themselves showed a clear sinusoidal pattern for low repetition rates, and the dynamic range even increased with lower repetition rates. For the highest repetition rates that did not elicit any response, the dynamic range was around zero but reached around 10° for the lowest two repetition rates. Analyzing the stimulus triggered average (STA) of eye position for all repetition rates revealed a phase shift with regard to stimulus position, which moved from positive phase angles towards negative ones with decreasing repetition rates (Figure 3D). For high repetition rates (0.25 and 0.5 Hz), the eyes therefore seemed to lag behind the stimulus, which is expected. For lower repetition rates (0.0078 to 0.125 Hz), however, eye movement preceded stimulus position change, which is counterintuitive. In other words: the eyes already started moving in the opposite direction during the slow-down of the current stimulus (before the sign of the stimulus velocity would change). For the highest repetition rate with responses (0.5 Hz), the phase lag was 65.76 ° ± 13.31 °, while for the lowest repetition rate (0.0078 Hz), the phase lag was -59.37 ° ± 15.69 ° (i.e. a phase advance). When analyzing those phase advances with regard to the eye's acceleration, we found that the sign of eye velocity only changed during slow-down of the stimulus, i.e. after the acceleration turned negative (Figure 2D, right panel). This phenomenon can potentially be explained by the motion aftereffect and will be further discussed.

The vOKR to a repetition rate of 0.125 Hz had the smallest phase lag and was used to investigate the tuning to spatial frequency. The angular velocities and spatial frequencies were varied following the constant rotation stimulus protocol. The dynamic range of vertical eye movements during sinusoidal vOKR overall revealed a similar pattern compared to the constant rotating stimulus (Figure 3E). On average, the dynamic range of eye position was small for high spatial frequencies, then began increasing and after peaking at 0.041 cyc/° or

0.061 cyc/°, it declined again for lower spatial frequencies. The maximum dynamic range for the slowest angular velocity (5.55 °/s) was 3.31 ° ± 2.44 °, and the maximum dynamic range for the fastest angular velocity (28.12 °/s) was 6.21 ° ± 3.02 °. When examining individual fish, much higher dynamic ranges, up to >10 ° (red dashed lines, Figure 3E) occurred in some fish. Two fish exhibited very distinct dynamic range tuning properties that stood out from the rest (purple and blue dashed lines). For high spatial frequencies, their dynamic range was much smaller (<1°) than the others. Furthermore, their maximum dynamic range for slower angular velocities was also relatively small, only starting to match the others as angular velocities increased.

The tuning of vOKR to spatial frequency and temporal frequency was similar for sinusoidal and constant rotation stimuli. The overall gains were higher for the sinusoidal rotation stimulus, though, reaching a maximum gain of 0.23 ± 0.03 (at 5.55 °/s and 0.041 cyc/°) and a more pronounced difference between 5.55°/s and 8.33°/s angular velocity (Figure 3F).

Zebrafish larvae generate pure vertical, pure horizontal, as well as vertical-horizontal saccades irrespective of the type of stimulus

In our recordings, saccadic eye movements were often detected simultaneously in the horizontal and in the vertical eye trace, no matter whether the fish was performing hOKR or vOKR. Overall, four different types of saccades could be classified, displaying the range of horizontal and vertical saccadic interplay (Figure 4A). Saccades either occurred only as vertical (cluster 1) or horizontal (cluster 2) eye movements, or vertical and horizontal saccades did together move in the same direction (CW or CCW, cluster 3) or in the opposite direction (CW and CCW, cluster 4). In total, 4696 detected saccades were analyzed during vOKR and could be assigned to one of the four clusters (Fig. 4B). Around 74% of all saccades consisted of simultaneous vertical and horizontal eye movements into the same direction (cluster 3).

The amplitude of cluster 3 saccades ranged from small movements up to more than 30°, with both vertical and horizontal components following linear relations with multiple slopes. Generally, the vertical and horizontal deflections of these saccades were either both high or both low. However, there were many cluster 3 saccades that did not follow this pattern, where the vertical amplitude was small even though the horizontal amplitude was large (black cloud of data points in Figure 4B). Cluster 1 and 2 saccades, which were detected only in the vertical

or horizontal eye trace, respectively, were observed much less often (only vertical: 477 ≙ 10.2 %; only horizontal: 658 ≙ 14.0 %).

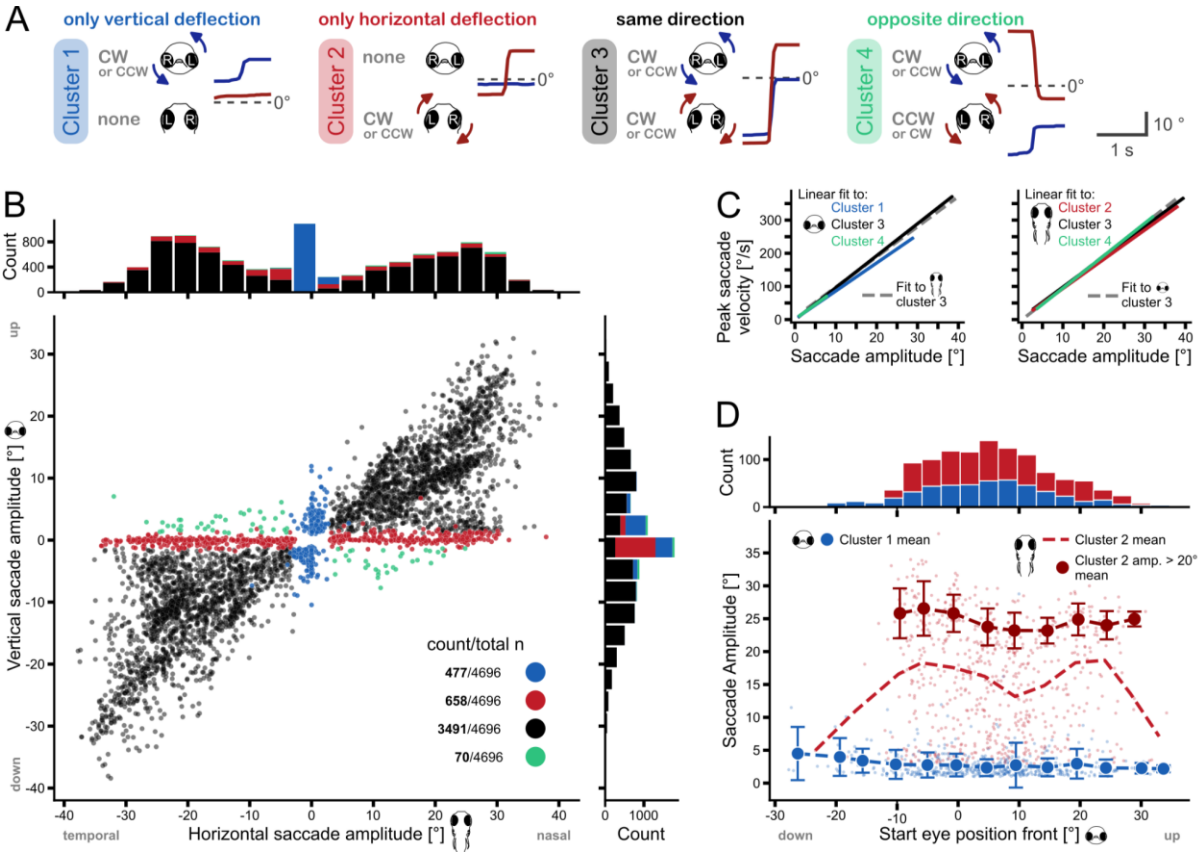

Figure 4: Pure vertical, pure horizontal, and mixed saccades do occur during visual roll stimulation. (A) Four different saccade types have been observed and can be distinguished by their vertical and horizontal contributions. **(B)** Scatterplot of horizontal and vertical amplitudes of all observed saccades clustered by the saccade type. **(C)** Linear fits to the relation of peak saccade velocity and saccade amplitude for every cluster. Left: vertical peak saccade velocity and saccade amplitude, dashed line for reference indicates the linear fit to the horizontal component of cluster 3. Pearson correlation coefficients: cluster 1: r=0.934, p<0.001; cluster 3: r=0.980, p<0.001; cluster 4: r=0.944, p<0.001. Right: horizontal peak saccade velocity and saccade amplitude, dashed reference line indicates the linear fit to the vertical component of cluster 3. Pearson correlation coefficients: cluster 2: r=0.974, p<0.001, cluster 3: r=0.965, p<0.001, cluster 4: p=0.981, r<0.001. **(D)** Relationship between front eye position at start of saccade and corresponding vertical and horizontal saccade amplitude for cluster 1 (pure vertical) and cluster 2 (pure horizontal). Blue circles and error bars show mean and standard deviation of binned cluster 1 saccades. Red circles and error bars show mean and standard deviation of cluster 2 saccades with amplitude larger than 20 °. Dashed lines indicate binned mean of all cluster 2 saccades.

Pure vertical saccades almost never exceeded 10° in magnitude but often had a small horizontal deflection of a few degrees. In contrast, pure horizontal saccades had virtually no vertical component. The key difference between pure vertical (cluster 1, blue) and pure

horizontal (cluster 2, red) saccades was their amplitude distribution. Horizontal only (cluster 2) saccade amplitudes were evenly distributed between small and large deflections, reaching over 30°, similar to the horizontal amplitudes of cluster 3 saccades. Cluster 1 saccades, however, only reached about 10° vertically, and their amplitudes were not evenly distributed between 0 and 10° but rather followed a bell-shaped pattern, with many small amplitude saccades and few larger amplitude ones. Only 70 saccades (≙ 1.5 %) were identified as cluster 4 saccades, characterized by horizontal and vertical eye deflections in opposite directions. The vertical amplitudes of these cluster 4 saccades rarely exceeded 5°, while their horizontal amplitudes reached magnitudes of over 30° (Figure 4B).

The main sequence of vertical and horizontal eye movements during vOKR displayed a similar linear profile across all clusters. Saccades with low amplitudes exhibited lower peak velocities, while those with larger amplitudes reached much higher peak velocities. The only exception was the vertical main sequence of cluster 1 (vertical only saccades), which appeared less steep compared to the other vertical and horizontal clusters (Figure 4C). Note that we were not able to record the actual maximal saccade velocity due to our low camera sampling rate.

To better understand whether saccade amplitude depended on the initial vertical eye position (down/ventral to up/dorsal) from where the saccade started, pure vertical and horizontal saccades (cluster 1 and 2) were further analyzed by plotting the saccades based on their vertical starting eye position (Figure 4D). For pure vertical saccades, the amplitude was equally small across all start positions. However, a slight trend was observed, suggesting that saccades starting at a more ventral eye position had slightly larger amplitudes than those with a more dorsal start position. Also, most saccades, no matter whether they were classified as cluster 1 or 2, occurred during more dorsal start position leading to a shift of the corresponding distribution. Most of the pure horizontal saccades (cluster 2) occurred between vertical start positions of -5° (ventral) and +20° (dorsal), and on average, amplitudes were a little smaller for extreme vertical start positions around +10° (dorsal). Nevertheless, horizontal cluster 2 saccades with an amplitude larger than 20° were equally distributed across all vertical start positions.

Interestingly, all four saccade types with similar distributions could also be observed during hOKR experiments.

Comparison of vOKR, hOKR and vVOR performance levels

Our findings are summarized in the comparison chart in Figure 5. Comparing the vOKR and vVOR is especially intriguing, as both involve the same extraocular eye muscles but are driven

by different sensory inputs. While resetting saccades are a characteristic feature of the hOKR, they did not occur during the vOKR or vVOR. Interestingly, spontaneous saccades were regularly observed in both directions (against and with stimulus direction) during the vOKR, whereas no saccades were present during the vVOR. This suggests that the vestibular roll stimulation or vVOR suppresses spontaneous saccadic eye movements (Figure 5A).

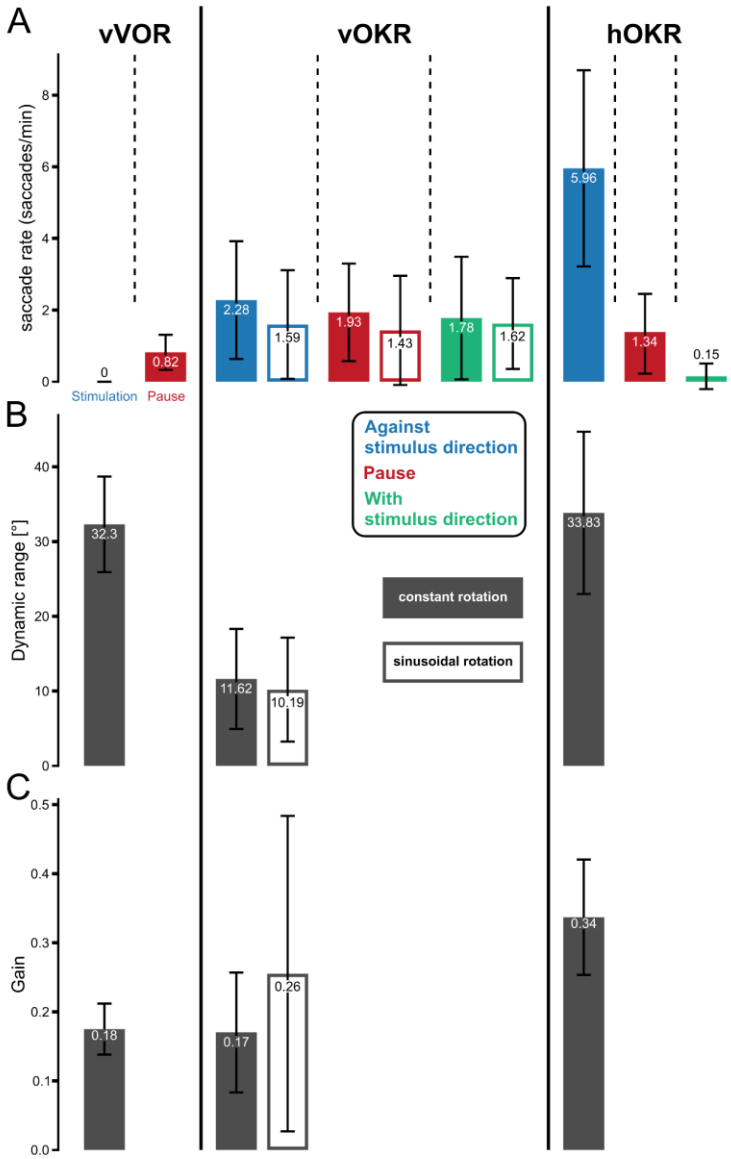

Figure 5: Performance comparison between vertical OKR, VOR and horizontal OKR. (A) Comparison of the saccade rate. For vVOR, data of recordings with the best response are shown. For vOKR and hOKR, data of all recordings irrespective of the stimulus parameters is shown. Red bars indicate saccade rate during static pauses in between stimuli. Blue bars indicate saccade rate of resetting saccades (against stimulus direction). Green bars indicate saccade rate of saccades in stimulus direction. **(B)** Comparison of the dynamic range. For all stimuli, data of recordings with stimulus parameters that elicited the highest dynamic range were used. For constant rotation (vOKR and hOKR) double the one directional amplitude was used as dynamic range. **(C)** Comparison of the gain (ratio of eye position to stimulus position after 4 s). For all stimuli, data of recordings with stimulus parameters

that elicited the highest gain are shown. All bars show mean values with standard deviation. For vOKR, filled bars represent values for the constant rotation stimulus whereas open bars represent values for the sinusoidal rotation stimulus.

To better understand the limits and maximal capabilities of the OKR and VOR, we compared the dynamic range and gain across the different reflexes (Figure 5B). While the dynamic range for both constant rotation and sinusoidal vOKR was around 10°, the dynamic range for vVOR was about three times larger. This striking difference indicates that the vertical deflection range utilized during vOKR is not limited by the maximum possible vertical oculomotor range of the plant. However, the dynamic range of vVOR and hOKR reached similar levels. The gain values for vOKR and vVOR were similar but were slightly higher for hOKR (Figure 5C).

Discussion

This study provides the first characterization of the vOKR in larval zebrafish and compares it to the hOKR and the vVOR. While hOKR has been intensively studied in zebrafish, the vOKR performance remained elusive, even though vertical and torsional OKR have been well-described in various species like primates, cats and even rabbits, which are also lateral-eyed animals, and like zebrafish do not have foveate vision [2–5,33]. Since zebrafish serve as a model system for vertebrate visuomotor circuitry, it is essential to know the full behavioral repertoire of the fish. By employing a novel experimental setup, we were able to track both horizontal and vertical eye movements simultaneously while the fish was presented with vertically or horizontally rotating visual stimuli.

Low vOKR performance levels

In mammals, both the hOKR and vertical vOKR consist of slow phases where the eye follows the stimulus, and resetting quick phases during which the eye rapidly moves in the opposite direction to allow for another slow phase [2,34–36]. Our vOKR experiment with a constant rotation stimulus, zebrafish revealed a markedly different response pattern. During the first seconds of stimulation, the fish vertically rotates its eyes in the direction of the stimulus. However, after reaching a certain degree of deflection, the eyes do not move further and do not perform any resetting saccades. This contrasts sharply with the behavior observed in mammals. Moreover, the zebrafish performs spontaneous saccades at regular intervals during vOKR stimulation, often with a horizontal component. This lack of suppression of spontaneous saccade generation during vOKR is in striking contrast to the vVOR, where not a single saccade occurred during vestibular stimulation. While the vOKR is highly robust in humans, in rabbits

it appears to be less effective than the hOKR, with fewer and more irregular resetting saccades, where the eyes often remained at their maximum deflection for over 10 seconds [2].

Generally, the OKR is used to compensate for low-frequency rotations, while the vestibulo-ocular reflex is used for high-frequency rotations of the body [36,37]. This principle could also apply to the vertical domain of the zebrafish sensory-motor systems, although we did not explicitly test it in this study and used different speed regimes for vVOR and vOKR stimulation. We speculate that the vOKR is presumably more relevant for slow and low-frequency roll rotations. Body rotations around this axis probably occur less frequently and with lower velocity amplitudes and dynamic ranges than for the yaw axis that elicits the hOKR. Such roll rotations would be quickly adjusted by the gravity-guided posture control mechanisms[20], which leaves no need for vertical resetting saccades, and a small-amplitude vOKR would be sufficient. Constant visual roll rotation should be very uncommon in healthy fish, which mainly modulate body yaw and - to a lesser extent - body pitch during swimming and navigation. [32,38,39].

Saccades during visual stimulation could be classified into four clusters based on their vertical and horizontal components. Although there are some uncertainties regarding the reliability of the combined horizontal and vertical saccades (cluster 3 and 4, see below), the presence of pure vertical and pure horizontal saccades (clusters 1 and 2) alone demonstrates that zebrafish larvae can precisely control their eye muscles to generate saccades with specific vertical and horizontal components. Interestingly, all four types of saccades were equally observed during both vOKR and hOKR experiments, although OKR performance and saccade rate was much higher for hOKR. The vertical saccades during yaw rotation stimuli likely are spontaneous (i.e. not directly driven by the stimulus). The horizontal resetting saccades during hOKR (quick phases) oftentimes had a vertical component. Further studies are needed to investigate the role of combined vs. pure horizontal and vertical saccades for zebrafish task performance and to reveal the ontogenetic performance levels of older larvae and adult zebrafish. Notably, the transient vOKR during constant rotation displayed a spatial frequency and angular velocity tuning that was highly similar to that previously observed for the hOKR [16,18].

The absolute peak gain values differed from a previous study though, with the reported hOKR having about four-times higher gain levels than our vOKR reported here[16]. The dynamic range was significantly different between the vertical and horizontal OKR, with the hOKR reaching much larger eye positions. This is particularly interesting given that during the vVOR, zebrafish were able to achieve three-times absolute higher vertical eye positions than during vOKR. Together with the high initial vOKR gain and the reported vertical motion sensitivity in the pretectum [27], these findings suggest that the limiting factor for vOKR is neither visual motion

sensitivity nor the oculomotor plant. Instead, these results point towards the inability of diencephalic direction-selective neurons in recruiting high levels of motoneuron pool activity needed for very peripheral eye positions. This could be caused by motoneurons with high eye position thresholds only being recruited by vestibular and not by visual input [40,41] or by the presence of saccade-type specific motoneuron populations [40,42,43].

Phase advances during low repetition rates might be related to adaptation

Using the sinusoidal rotation stimulus, it was possible to evoke a long-lasting sinusoidal vOKR that followed the stimulus position. For low repetition rates that affected extended periods of unidirectional stimulus motion, the eyes reached their maximum vertical deflection already after several seconds and remained at that plateau. One might expect the eyes to stay at the plateau until the stimulus changed direction, at which point the eyes would move in the opposite direction away from the plateau. However, the eyes appeared to start rotating in the opposite direction several seconds before the stimulus changed direction, i.e. the stimulus was still moving in the original direction (just slower). This was true for all repetitions during a stimulation phase and did not evolve over time, which is why predictive behavior occurring after a training period with a repetitive stimulus can be ruled out [44,45].

This phenomenon shares some similarities with the motion aftereffect (MAE), an illusion of motion in a certain direction caused by prior exposure to motion in the opposite direction [46]. The motion aftereffect can reliably be elicited by moving visual stimuli [47–49] and is also known to be present in larval zebrafish with regard to both the optomotor and optokinetic response [50–53]. After prolonged hOKR stimulation, fish exhibit a hOKR in the opposite direction during a stationary stimulus, and the duration of the reversed response depends on the duration of the initial stimulation. At least 200 seconds of hOKR stimulation is necessary to induce a MAE [51]. Two key differences to the behavior observed in this study are that i) zebrafish began moving their eyes in the opposite direction while the stimulus was still moving, and ii) that our observed phase-advanced vOKR occurred for stimulation periods much shorter than 200 seconds. For the lowest repetition rate, the duration of stimulus rotation in one direction was over 2 minutes, whereas for a repetition rate of 0.125 Hz, the stimulus rotated for only 4 seconds in one direction, and a small phase advance was already visible. One potential explanation for the occurrence of the phase advance could be an interplay between two mutually inhibiting populations of direction-selective (DS) neurons coding for opposite velocities. The population coding for the stimulus direction may adapt over time, until the difference between the two population's activities is so small that a deceleration of the stimulus disinhibits the non-

stimulated DS population, which induces a vOKR in the opposite direction. However, the fast adaptation (< 4 s for 0.125 Hz repetition rate) is much faster than previously reports on MAE in zebrafish [51,53].

An alternative explanation for the occurrence of phase advances is that the DS neurons - next to their tuning to velocity - are tuned to acceleration as well [54,55], which can be interpreted as a quick form of adaptation, and thus they might lose much of their activity when the stimulus is still running in the same direction but acceleration went missing. In this scenario, the occurring eye movements into the opposite direction (back to the null position) would not necessarily be visually driven, but could simply result from passive drift back of the eyes in the oculomotor plant [56]. In line with this hypothesis, centripetal eye movements (which can be interpreted more safely as visually driven) only occurred after the stimulus velocity had switched sign (Fig. 3D), i.e. vOKR towards peripheral positions was always going in the same direction as the stimulus.

Further studies are needed to determine the mechanisms that underly the observed phase advance of vertical optokinetic responses to slowly repeating sinusoidal rotation stimuli.

Uncertainties associated with projection-based eye tracking

The dual-camera setup used for all recordings enabled a novel simultaneous tracking of horizontal and vertical eye movements in zebrafish larvae. However, many eye movements were visible in both horizontal and vertical eye traces. In particular, saccades with large amplitudes were often visible in both cameras. We tracked horizontal eye movements in larval zebrafish by fitting an ellipse to the binarized eye image and calculating the angle between the major axis and the body midline. This method should be relatively robust as compared to a previously reported method based on searching the largest distance of two pixels within a binarized and segmented eye[57]. However, our approach might still produce biased eye position readings as we don’t know the exact 3D-shape of the eye and how its projection is affected by the fish body. Inspection of the raw video material revealed that large horizontal eye movements influenced the shape of the eye projection onto the front camera, often resulting in an ellipse fit with a major/minor axis ratio closer to a value of one than for eye positions without horizontal components, and this change in projection shape potentially affected the calculated vertical angle. The change in projection shape in the frontal camera was especially apparent during hOKR recordings, where the stereotypical slow/quick phase pattern was also observed in the vertical eye trace, albeit with a much smaller amplitude. If these eye movements were genuine, it would suggest that the hOKR has a constant vertical

component, which would be surprising, even when considering the potential for small body pitch due to imprecise embedding of the larva.

The presence of cluster 2 saccades, which had only a horizontal component and were not visible in the front camera, together with the good separation of cluster 2 and cluster 3 in Fig. 4B suggest that pure horizontal saccades do exist. Many of the spontaneous saccades observed during vOKR had horizontal and vertical components with the same directionality, indicating that those might primarily be horizontal saccades. Interestingly, the vertical component of saccades with both horizontal and vertical components but with opposing directions (cluster 4) exhibited maximum amplitudes of about 10°. This value also roughly matches the saccade amplitude that was reached for saccades with solely vertical components and the dynamic range achieved during vOKR. These observations suggest that saccades where the vertical and horizontal directions were opposite to each other comprised a true vertical component. Taken together, our data shows that pure horizontal and pure vertical saccades do exist, as well as mixed horizontal-vertical saccade types. The precise measurement of vertical components in individual horizontal-vertical saccades is hampered by methodological caveats, though, and a more elaborate analysis of the dual-camera recordings needs to be performed in the future to improve our understanding of the horizontal and vertical components of saccades in larval zebrafish.

Conclusion

In this study, we characterized the vOKR in larval zebrafish and compared its characteristics to the hOKR and the vVOR. Larval zebrafish do perform vOKR and several basic differences from the hOKR could be identified. One major difference was the absence of resetting vertical saccades during vOKR. The reason for this needs to be explored in future studies. Given that vertical rotation encoding neurons exist [27,31], a better understanding of the downstream neuronal processes controlling eye movement and saccade generation could help explain the behavioral differences between vertical and horizontal OKR. Such neurophysiology experiments could also shed light on the differences in dynamic range between vOKR and the vVOR. Additionally, further behavioral experiments are necessary to understand the apparent vOKR phase advance for sinusoidal rotation stimuli in the context of adaptation or acceleration tuning. Our characterization of the vOKR in larval zebrafish opens up numerous avenues for future research to gain a more comprehensive understanding of the neuronal processing of visual information and the control of eye movements.

Methods

Animals

Animal experiments were permitted by the local government authorities (Regierungspraesidium Tuebingen) and conducted in accordance with German federal law and Baden-Württemberg state law. Zebrafish larvae (*Danio rerio*) were reared on a 14/10 h light/dark cycle at 28°C in E3 medium (5 mM NaCl, 0.17 mM KCl, 0.33 CaCl, 0.33 MgSO4) with 0.01% methylene blue. All experiments were performed on 4 dpf zebrafish larvae which are known to reliably perform OKR [15].

Setup for VOR Experiments

To examine vertical eye movements of the vestibular ocular reflex (VOR), a setup named KEBAB (Kinematic Evaluation of Behavior during Animal Body-roll) with the ability of rotating a single larva around its rostral-caudal axis (roll) was developed and built in-house. For the most parts, standard Thorlabs components were used to build an examination chamber, IR-illumination for eye-tracking, visual stimulation and a camera path - all on a single axis using the 30 mm Thorlabs cage system. A Nema 17 stepper motor (ACT Motor GmbH, Germany) was used to rotate the whole setup. To provide electricity and enable data transfer from the steady world to the rotating camera system, its USB cable was connected via a rotating electrical slip ring (BQLZR 0.48” 12 Wire 2A 240V, Amazon). Both IR-illumination and visual stimulation consisted of LED-diodes (850nm and white) with a 120-grid diffuser to provide uniform illumination. For examination, larvae were embedded on a triangle stage in 1.6% low melting agarose as described in Wang et al. [28]. Agarose around the eyes was removed to allow ocular movements. The stage was then clipped to a custom-made 3D-printed mount. The whole KEBAB setup was operated via an Arduino Uno with an A4988 RepRap stepper motor driver and the Python library Telemetrix (https://mryslab.github.io/telemetrix/) to enable remote control via a PC. The custom written Python-based software vxPy (https://github.com/thladnik/vxPy) was used to control setup rotation, visual stimulus presentation, camera recording and eye tracking.

To investigate the vertical VOR, a stimulus protocol consisting of 2 x 3 stimulation phases, each framed by a 30 s pause phase was conducted in complete darkness. During the stimulation phases, the KEBAB performed 8 full rotations at either 90°/s, 45°/s or 22.5°/s velocity in either clockwise or counter-clockwise direction. Both directions were performed for each head rotation velocity. During the pause phases no rotation was performed.

Data Analysis of VOR Experiments

First, all eye traces of stimulation phases were smoothed using a rolling mean filter with a window size of 2 s and centered around a 0°-axis to get rid of noise and outliers. VOR score was calculated similar to Sun et al. 2018 [58] by Fourier-transforming all eye traces into the power spectrum and then taking the amplitude at the head's rotation frequency (0.25, 0.125, 0.0625 Hz) in degree as the corresponding score. For gain and phase shift calculation, a sine-function was fitted to the stimulus triggered average (STA) of eye positions to get the full amplitude of eye movements. Gain was then calculated as the ratio between the amplitude of eye movement and the corresponding head position, similar to Dehmelt et al. [18]. Phase shift was calculated by using cross-correlation.

All significant differences between different head rotation velocities were determined by a paired t-test followed by Bonferroni correction.

In our vVOR experiments, we only used a single front camera, and in the vOKR experiments, we noticed that many horizontal eye movements occurred during vOKR. We therefore carefully inspected the vVOR videos and are confident that no major horizontal eye movement components occurred. This observation is mainly based on the continuous visibility of the eye lens protruding on the side in the projected front camera recording.

Setup for vOKR and hOKR Experiments

For recording horizontal and vertical optokinetic response (OKR) behavior, a modified version of the visual stimulation arena described in Dehmelt et al. (2018) [57] was used. To record horizontal and vertical eye movements simultaneously, the stimulation displays in front and at the back of the fish were removed. An additional camera was positioned in front of the fish additionally to the camera from the top and the corresponding infrared (IR) backlight was positioned behind the fish. Fish were positioned in the middle of the arena in a water-filled translucent container and the cameras were adjusted so that both had a good view on the head and the eyes of the fish. A black lid was placed onto the container making sure that it had direct contact to the water surface to prevent unwanted reflections at the water-air surface. A similar cover was placed on the bottom of the container for the same reason. Both lid and bottom cover had a small hole in the middle to allow the IR bottom backlight to reach the fish and the camera from the top to see the fish. The two remaining displays on the left and the right side of the fish were used for OKR stimulus presentation and were sufficient to elicit OKR behavior. For each recording, a single zebrafish larva was embedded into 1.6% agarose. The procedure was similar to that described for the vVOR experiments, but to enable both vertical

and horizontal eye movements along with high-quality video recording in the IR spectrum, the agarose around the eyes was removed, leaving a small triangular portion to stabilize the head.

vOKR and hOKR Stimulus Protocols

To assess whether zebrafish larvae exhibit a vOKR and characterize its tuning to different stimulus parameters, a constant rotation OKR stimulus was used. To characterize the vOKR tuning, stimulus parameters known to encompass the range of best hOKR tuning were adapted from Dehmelt et al. (2021) [18]. All possible combinations of six different spatial frequencies and five different angular velocities were tested. The stimulus protocol consisted of alternating stimulation phases where the stimulus would rotate in either clockwise or counter-clockwise direction, framed by 60 s pause phases with a static grating. The order of spatial frequency and angular velocity pairs was randomized for each recording, as well as the direction of rotation, with each parameter pair rotating clockwise and counter-clockwise, respectively.

Since larvae only responded within the first few seconds to a constant rotating stimulus, a second stimulus protocol using sinusoidally modulated rotation was designed with the aim of eliciting a more robust and prolonged vOKR. The number of stimulus periods within one second is defined as the repetition rate. First, vOKR tuning to 10 different repetition rates was examined, holding the angular velocity and spatial frequency constant at 12.5°/s and 0.0611 cyc/°, respectively. Each repetition rate was displayed twice in a randomized order and with randomized directions, with one stimulation phase consisting of 6 stimulus periods. Stimulation phases were framed by 20 s pause phases with a static grating.

After characterizing the vOKR tuning to repetition rate, the vOKR tuning to angular velocity and spatial frequency was assessed, using the same parameter range as for the constant rotating stimulus protocol with the sinusoidal modulation at repetition rate of 0.125 Hz.

Data Analysis of vOKR Experiments

All eye traces were filtered with a median filter with a window size of 1 s to remove noise while preserving the velocity profile of the saccadic eye movements. Saccadic eye movements were detected using a multi-step process, including identifying the start and end points of each saccade based on the first and second derivatives of the eye traces. A threshold of 1° minimal deflection and a threshold of 30°/s or 10°/s peak velocity during saccadic movements (for horizontal and vertical eye movements respectively) were applied, with the values selected based on visual inspection of the data. Also, the overall duration of saccade must not exceed 0.5 s. If multiple potential start and end points were detected for a single saccade, a scoring

system was used to select the most appropriate ones. This was the same for both recordings using the constant and sinusoidal rotating stimulus. After start and end timepoints of each saccade had been determined in a last step, the frames before and after both start and endpoint were screened for eye deflection differences. If in the frame before or after start or end a more extreme eye deflection was reached that exceeded 0.5 °, the timepoint for start or end was shifted to the frame with the eye trace extremum. Saccades were detected individually for each eye and camera.

The gain during the constant rotating stimulus was calculated by taking the ratio of the eye deflection within the first four seconds of each stimulation phase to the corresponding stimulus position. Cumulative average eye positions were calculated by removing all saccades and then averaging all eye traces across all stimulation phases. This same process was applied to the first 15 seconds, but without removing saccades, to better illustrate the initial vertical response.

Recordings performed alongside the sinusoidal rotating stimulus were often disrupted by spontaneous saccades, although showing an overall sinusoidal pattern. A combined Wiener and median filter were applied to remove high-frequency eye movements, and the signal was detrended afterwards. All further analysis was done using the average response to one stimulus period (stimulus triggered average - STA). Eye response periods where 50% of all data points exceeded the standard deviation over all other periods within the same stimulation phase were removed from the STA to account for potential distortions by left over saccades. Gain was calculated by taking the ratio of a peak-to-peak sine function fitting over the STA and the peak-to-peak stimulus position (similar to Dehmelt et al. (2021)[18]). Dynamic range was calculated as the difference between the maximum and minimum eye positions of the STA. The top of descent (ToD), used for analyzing phase shifts, was defined as the point where a rolling mean of the STA gradient decreased by half of the standard deviation after the peak of the sine curve. The ToD shift was then calculated as the difference between the ToD of the stimulus and the ToD of the STA.

References

1. Land, M. F. Eye movements of vertebrates and their relation to eye form and function. *J. Comp. Physiol. A* **201**, 195–214 (2015).
2. Erickson, R. G. & Barmack, N. H. A comparison of the horizontal and vertical optokinetic reflexes of the rabbit. *Exp. Brain Res.* **40**, 448–456 (1980).
3. van den Berg, A. V. & Collewijn, H. Directional asymmetries of human optokinetic nystagmus. *Exp. Brain Res.* **70**, 597–604 (1988).
4. Kitama, T., Ishida, M., Luan, H., Kawasaki, T. & Sato, Y. Difference between Horizontal and Vertical Optokinetic Nystagmus in Cats at Upright Position. *Jpn. J. Physiol.* **51**, 463–474 (2001).
5. Farooq, S. J. Torsional optokinetic nystagmus: normal response characteristics. *Br. J. Ophthalmol.* **88**, 796–802 (2004).
6. Matsuda, K. & Kubo, F. Circuit Organization Underlying Optic Flow Processing in Zebrafish. *Front. Neural Circuits* **15**, (2021).
7. Orger, M. B. The Cellular Organization of Zebrafish Visuomotor Circuits. *Curr. Biol.* **26**, R377–R385 (2016).
8. Kasprick, D. S. *et al.* Microanatomy of Adult Zebrafish Extraocular Muscles. *PLOS ONE* **6**, e27095 (2011).
9. Bellegarda, C., Auer, F. & Schoppik, D. Zebrafish as a model to understand extraocular motor neuron diversity. *Curr. Opin. Neurobiol.* **90**, 102964 (2025).
10. Takabayashi, A., Ohmura-Iwasaki, T. & Mori, S. Changes of vertical eye movements of goldfish for different otolith stimulation by linear acceleration. *Adv. Space Res.* **32**, 1527–1532 (2003).
11. Beck, J. C., Gilland, E., Tank, D. W. & Baker, R. Quantifying the Ontogeny of Optokinetic and Vestibuloocular Behaviors in Zebrafish, Medaka, and Goldfish. *J. Neurophysiol.* **92**, 3546–3561 (2004).
12. Lambert, F. M., Beck, J. C., Baker, R. & Straka, H. Semicircular Canal Size Determines the Developmental Onset of Angular Vestibuloocular Reflexes in Larval Xenopus. *J. Neurosci.* **28**, 8086–8095 (2008).
13. Lim, K. H. *et al.* Measuring Optokinetic Reflex and Vestibulo-Ocular Reflex in Unilateral Vestibular Organ Damage Model of Zebrafish. *J. Assoc. Res. Otolaryngol.* **25**, 167–177 (2024).
14. Bollmann, J. H. The Zebrafish Visual System: From Circuits to Behavior. *Annu. Rev. Vis. Sci.* **5**, 269–293 (2019).
15. Easter Jr., S. S. & Nicola, G. N. The development of eye movements in the zebrafish (Danio rerio). *Dev. Psychobiol.* **31**, 267–276 (1997).

16. Rinner, O., Rick, J. M. & Neuhauss, S. C. F. Contrast Sensitivity, Spatial and Temporal Tuning of the Larval Zebrafish Optokinetic Response. *Invest. Ophthalmol. Vis. Sci.* **46**, 137–142 (2005).
17. Huang, Y.-Y. & Neuhauss, S. C. F. The optokinetic response in zebrafish and its applications. *Front. Biosci.-Landmark* **13**, 1899–1916 (2008).
18. Dehmelt, F. A. *et al.* Spherical arena reveals optokinetic response tuning to stimulus location, size, and frequency across entire visual field of larval zebrafish. *eLife* **10**, e63355 (2021).
19. Bianco, I. H. *et al.* The Tangential Nucleus Controls a Gravito-inertial Vestibulo-ocular Reflex. *Curr. Biol.* **22**, 1285–1295 (2012).
20. Sugioka, T., Tanimoto, M. & Higashijima, S. Biomechanics and neural circuits for vestibular-induced fine postural control in larval zebrafish. *Nat. Commun.* **14**, 1217 (2023).
21. Ben-Simon, A., Ben-Shahar, O. & Segev, R. Measuring and tracking eye movements of a behaving archer fish by real-time stereo vision. *J. Neurosci. Methods* **184**, 235–243 (2009).
22. Graf, W. & Meyer, D. L. Central mechanisms counteract visually induced tonus asymmetries. *J. Comp. Physiol.* **150**, 473–481 (1983).
23. Warren, W. H. & Hannon, D. J. Direction of self-motion is perceived from optical flow. *Nature* **336**, 162–163 (1988).
24. Britten, K. H. Mechanisms of Self-Motion Perception. *Annu. Rev. Neurosci.* **31**, 389–410 (2008).
25. Festl, F., Recktenwald, F., Yuan, C. & Mallot, H. A. Detection of linear ego-acceleration from optic flow. *J. Vis.* **12**, 10 (2012).
26. Kubo, F. *et al.* Functional Architecture of an Optic Flow-Responsive Area that Drives Horizontal Eye Movements in Zebrafish. *Neuron* **81**, 1344–1359 (2014).
27. Wang, K., Hinz, J., Haikala, V., Reiff, D. F. & Arrenberg, A. B. Selective processing of all rotational and translational optic flow directions in the zebrafish pretectum and tectum. *BMC Biol.* **17**, 29 (2019).
28. Wang, K., Hinz, J., Zhang, Y., Thiele, T. R. & Arrenberg, A. B. Parallel Channels for Motion Feature Extraction in the Pretectum and Tectum of Larval Zebrafish. *Cell Rep.* **30**, 442-453.e6 (2020).
29. Gabriel, J. P., Trivedi, C. A., Maurer, C. M., Ryu, S. & Bollmann, J. H. Layer-Specific Targeting of Direction-Selective Neurons in the Zebrafish Optic Tectum. *Neuron* **76**, 1147–1160 (2012).
30. Hunter, P. R., Lowe, A. S., Thompson, I. D. & Meyer, M. P. Emergent Properties of the Optic Tectum Revealed by Population Analysis of Direction and Orientation Selectivity.

J. Neurosci. **33**, 13940–13945 (2013).

31. Zhang, Y., Huang, R., Nörenberg, W. & Arrenberg, A. B. A robust receptive field code for optic flow detection and decomposition during self-motion. *Curr. Biol.* **32**, 2505-2516.e8 (2022).
32. Ehrlich, D. E. & Schoppik, D. Control of Movement Initiation Underlies the Development of Balance. *Curr. Biol.* **27**, 334–344 (2017).
33. Collewijn, H. Sensory control of optokinetic nystagmus in the rabbit. *Trends Neurosci.* **3**, 277–280 (1980).
34. Garbutt, S. *et al.* Vertical Optokinetic Nystagmus and Saccades in Normal Human Subjects. *Invest. Ophthalmol. Vis. Sci.* **44**, 3833–3841 (2003).
35. Ghasia, F. & Tychsen, L. Horizontal and Vertical Optokinetic Eye Movements in Macaque Monkeys With Infantile Strabismus: Directional Bias and Crosstalk. *Invest. Ophthalmol. Vis. Sci.* **55**, 265–274 (2014).
36. Robinson, D. A. The Use of Control Systems Analysis in the Neurophysiology of Eye Movements. *Annu. Rev. Neurosci.* **4**, 463–503 (1981).
37. Masseck, O. A. & Hoffmann, K.-P. Comparative Neurobiology of the Optokinetic Reflex. *Ann. N. Y. Acad. Sci.* **1164**, 430–439 (2009).
38. Budick, S. A. & O'Malley, D. M. Locomotor repertoire of the larval zebrafish: swimming, turning and prey capture. *J. Exp. Biol.* **203**, 2565–2579 (2000).
39. Mearns, D. S., Donovan, J. C., Fernandes, A. M., Semmelhack, J. L. & Baier, H. Deconstructing Hunting Behavior Reveals a Tightly Coupled Stimulus-Response Loop. *Curr. Biol.* **30**, 54-69.e9 (2020).
40. Brysch, C., Leyden, C. & Arrenberg, A. B. Functional architecture underlying binocular coordination of eye position and velocity in the larval zebrafish hindbrain. *BMC Biol.* **17**, 110 (2019).
41. Aksay, E., Baker, R., Seung, H. S. & Tank, D. W. Anatomy and Discharge Properties of Pre-Motor Neurons in the Goldfish Medulla That Have Eye-Position Signals During Fixations. *J. Neurophysiol.* **84**, 1035–1049 (2000).
42. Dowell, C. K., Hawkins, T. & Bianco, I. H. Subsets of extraocular motoneurons produce kinematically distinct saccades during hunting and exploration. *Curr. Biol.* **35**, 554-573.e6 (2025).
43. Leyden, C., Brysch, C. & Arrenberg, A. B. A distributed saccade-associated network encodes high velocity conjugate and monocular eye movements in the zebrafish hindbrain. *Sci. Rep.* **11**, 12644 (2021).
44. Miki, S., Baker, R. & Hirata, Y. Cerebellar Role in Predictive Control of Eye Velocity Initiation and Termination. *J. Neurosci.* **38**, 10371–10383 (2018).
45. Marsh, E. & Baker, R. Normal and Adapted Visuooculomotor Reflexes in Goldfish. *J.*

Neurophysiol. **77**, 1099–1118 (1997).

46. Anstis, S., Verstraten, F. A. J. & Mather, G. The motion aftereffect. *Trends Cogn. Sci.* **2**, 111–117 (1998).
47. Braun, D. I., Pracejus, L. & Gegenfurtner, K. R. Motion aftereffect elicits smooth pursuit eye movements. *J. Vis.* **6**, 1 (2006).
48. Chen, C.-C., Huang, M. Y.-Y., Weber, K. P., Straumann, D. & Bockisch, C. J. Afternystagmus in darkness after suppression of optokinetic nystagmus: an interaction of motion aftereffect and retinal afterimages. *Exp. Brain Res.* **232**, 2891–2898 (2014).
49. Watamaniuk, S. N. J. & Heinen, S. J. Storage of an oculomotor motion aftereffect. *Vision Res.* **47**, 466–473 (2007).
50. Najafian, M., Alerasool., N. & Moshtaghian, J. The effect of motion aftereffect on optomotor response in larva and adult zebrafish. *Neurosci. Lett.* **559**, 179–183 (2014).
51. Pérez-Schuster, V. *et al.* Sustained Rhythmic Brain Activity Underlies Visual Motion Perception in Zebrafish. *Cell Rep.* **17**, 1098–1112 (2016).
52. Lin, T.-F. *et al.* Negative optokinetic afternystagmus in larval zebrafish demonstrates set-point adaptation. *Sci. Rep.* **9**, 19039 (2019).
53. Wu, Y., dal Maschio, M., Kubo, F. & Baier, H. An Optical Illusion Pinpoints an Essential Circuit Node for Global Motion Processing. *Neuron* **108**, 722-734.e5 (2020).
54. Thiel, A., Greschner, M., Eurich, C. W., Ammermüller, J. & Kretzberg, J. Contribution of Individual Retinal Ganglion Cell Responses to Velocity and Acceleration Encoding. *J. Neurophysiol.* **98**, 2285–2296 (2007).
55. Cao, P., Gu, Y. & Wang, S.-R. Visual Neurons in the Pigeon Brain Encode the Acceleration of Stimulus Motion. *J. Neurosci.* **24**, 7690–7698 (2004).
56. Miri, A., Bhasin, B. J., Aksay, E. R. F., Tank, D. W. & Goldman, M. S. Oculomotor plant and neural dynamics suggest gaze control requires integration on distributed timescales. *J. Physiol.* **n/a**,.
57. Dehmelt, F. A., von Daranyi, A., Leyden, C. & Arrenberg, A. B. Evoking and tracking zebrafish eye movement in multiple larvae with ZebEyeTrack. *Nat. Protoc.* **13**, 1539–1568 (2018).
58. Sun, P. *et al.* An Assay for Systematically Quantifying the Vestibulo-Ocular Reflex to Assess Vestibular Function in Zebrafish Larvae. *Front. Cell. Neurosci.* **12**, (2018).

Author Contributions

D-S.B. and T.C.H. developed and built the setups, D-S.B., G.B and A.B.A. developed the methodologies. G.M., L.D. and C.F. recorded all data. D-S.B. and G.M. did the data analysis and made the figures. D.-S.B., A.B.A and G.M. wrote the manuscript. D.-S.B. and A.B.A. supervised the project.

Competing Interests

The authors declare no competing interests.